Fine Structure of Negatively and Positively Charged Excitons in Semiconductor Quantum Dots: Electron-Hole Asymmetry

M. Ediger,[1] G. Bester,[2] B. D. Gerardot,[1] A. Badolato,[3] P. M. Petroff,[3] K. Karrai,[4] A. Zunger,[2] and R. J. Warburton[1]

[1]*School of Engineering and Physical Sciences, Heriot-Watt University, Edinburgh EH14 4AS, United Kingdom*

[2]*National Renewable Energy Laboratory, Golden, Colorado 80401, USA*

[3]*Materials Department, University of California, Santa Barbara, California 93106, USA*

[4]*Center for NanoScience and Department für Physik, Ludwig-Maximilians-Universität, 80539 München, Germany*

(Received 26 June 2006; published 19 January 2007)

We present new understanding of excitonic fine structure in close-to-symmetric InAs/GaAs and InGaAs/GaAs quantum dots. We demonstrate excellent agreement between spectroscopy and many-body pseudopotential theory in the energy splittings, selection rules and polarizations of the optical emissions from doubly charged excitons. We discover a marked difference between the fine structure of the doubly negatively and doubly positively charged excitons. The features in the doubly charged emission spectra are shown to arise mainly from the lack of inversion symmetry in the underlying crystal lattice.

DOI: 10.1103/PhysRevLett.98.036808 PACS numbers: 73.21.La, 78.67.Hc

The symmetry of a quantum mechanical system determines the degeneracies of its states and has therefore important consequences for the physical behavior. In a semiconductor quantum dot, a departure from idealized symmetry completely changes the behavior as exemplified by its excitonic fine structure [1]. The promotion of an electron across the energy gap creates an exciton, an electron-hole pair. The exchange interaction between the electron and hole is sensitive to the symmetry and splits the main optical transition into a doublet with a typical separation of tens of μeV for InAs dots [1–3] with the two components of the doublet linearly polarized along the $[110]$ and $[1\bar{1}0]$ directions. The presence of this fine structure has profound consequences. On the one hand, it enables the realization of two-exciton entangled states with two laser pulses [4]; on the other hand however, it inhibits the generation of a polarization-entangled pair of photons when the two-exciton state decays [5–7]. However, despite the importance of these results for single-photon sources, entangled-photon sources, and exciton-based qubits, a quantitative understanding of the exciton fine structure, in particular its symmetry dependence, is presently lacking.

Describing the symmetry is complicated as the macroscopic dot shape and the underlying lattice are interwoven [3]. In almost all cases so far, quantum dot fine structure has been described with an effective Hamiltonian taking parameters from the bulk [8] or directly from experiment [1,9]. In the latter case, the calculations are not predictive but merely rephrase the experimental observation. Here, we interpret new spectroscopy results on single quantum dots within an atomistic theoretical framework. We concentrate on dots with a close-to-symmetric shape, focusing on the doubly charged excitons, X^{2-} ($1h + 3e$ complex) and X^{2+} ($3h + 1e$) as charging opens up new recombination pathways relative to the neutral exciton X^0 [10], affording a sensitive comparison between theory and experiment.

We performed spectroscopy experiments on two samples, one containing dots emitting around 1.05 eV (''InAs'' dots), the other dots emitting at 1.3 eV (''InGaAs'' dots). The InAs dots are In rich and lens shaped with a typical diameter of 25 nm and height 2 to 3 nm. The InGaAs dots are highly alloyed but with similar dot size. We can judge the shape symmetry of the dot from the splitting of the excited electron P orbitals. X^{3-} is sensitive to this splitting [11]: only for a small splitting is the open shell X^{3-} configuration favored over the closed shell configuration. The open shell X^{3-} photoluminescence (PL) has a characteristic signature, two lines split by electron-electron exchange [11]. For all the dots which show a clear X^{3-} (all the InAs dots and the majority of the InGaAs dots), the open shell is favored over the closed shell, implying a small, sub $\sim$2 meV, P shell splitting. This splitting is comparable to the splitting found theoretically for circularly symmetric dots [3]. Also, the fine structure splitting $\Delta_1(X^0)$ of the InGaAs neutral exciton in the band 1.29 to 1.31 eV is small with an average value (standard deviation) of 26(12) μeV [2], consistent with values calculated for circularly symmetric dots [3] but smaller than those reported recently [8,12]. In our case, both the small P shell splitting and the small $\Delta_1(X^0)$ point to a highly symmetric dot shape. The dots are embedded in a field-effect structure which allows controlled charging with both electrons and holes [13,14]. We measure the PL following nonresonant excitation at 850 nm, dispersing the PL with a grating spectrometer and Si (InGaAs) array detector for the InGaAs (InAs) dots. We measure the PL with linear polarization in the $[110]$ and $[1\bar{1}0]$ directions. The fine-structure splittings have no measurable dependence on electric field within a charging plateau. The FWHM of the spectral response to a narrow band source is 60(120) μeV at 1.3 (1.05) eV. By fitting Lorentzian line shapes to high signal-to-noise spectra we can determine peak positions with an accuracy of 10 μeV. Dot-to-dot

fluctuations were evaluated by measuring 10 dots from the InGaAs sample in the band 1.29–1.31 eV and a few InAs dots in the band 1.04–1.06 eV.

We have calculated the optical properties of both InAs and InGaAs quantum dots with the empirical pseudopotential method with a configuration interaction treatment of correlations [15]. The crystal potential is calculated as a superposition of atomic screened potentials v_α (of atom type α) at each relaxed atomic position $\mathbf{R}_{\alpha n}$ (where n is the lattice site index): $V(\mathbf{r}) = \sum_{\alpha n} v_\alpha(\mathbf{r} - \mathbf{R}_{\alpha n})$. The description of the dots and its wetting layer in terms of the set $\{\mathbf{R}_{\alpha n}\}$ guarantees that the symmetries are resolved even at the atomistic level. The Hamiltonian is solved in a single-particle basis consisting of multiple Bloch states spread throughout the Brillouin zone. We include piezoelectricity in our calculations using first and second order effects [16]. The few-particle states, excitons and charged excitons, are calculated using a configuration interaction approach, where the Coulomb and exchange integrals are calculated explicitly from the single-particle wave functions. The distinction between short-range and long-range, or between isotropic and anisotropic electron-hole exchange does not arise. We use the available geometrical and structural data on the real dots as input to the theory: we model lens-shaped 25 nm diameter $In_{0.6}Ga_{0.4}As$ and InAs dots sitting on 2 monolayers of wetting layer with heights 3.5 and 2 nm, respectively. The calculated X^0 emission energies are 1.25 and 1.07 eV, matching the experimental X^0 PL energies, suggesting that these structures are good representations of the real ones. While the macroscopic symmetry is $D_{\infty v}$, the real symmetry is reduced to C_{2v} by the atomistic symmetry of the zinc blende lattice, leading to the inequivalence of the [110] and $[1\bar{1}0]$ directions. The neutral exciton X^0 made of the fundamental electron (e_0) and hole (h_0) levels has four states: a lower dark doublet split slightly by band-mixing effects, and at energy Δ_0 above, a bright doublet split by Δ_1.

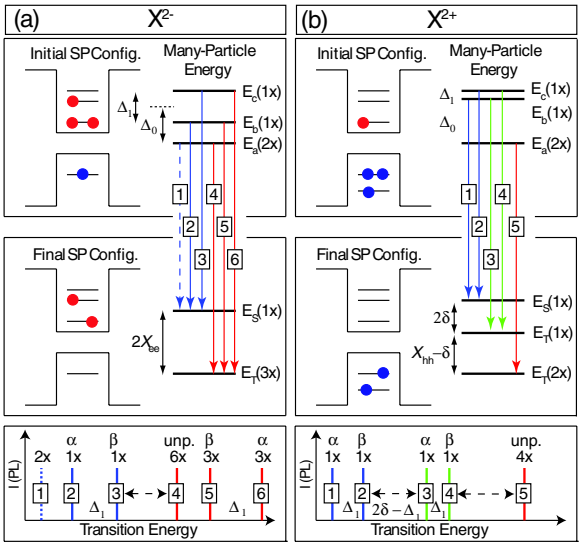

FIG. 1 (color online). Schematic of the calculated energy level diagram for (a) X^{2-}, and (b) X^{2+}. On the left of each panel we show the dominant initial and final single-particle (SP) configurations while the energy levels on the right correspond to many-body states. The spectra ensue from the many-body transitions and give the degree of degeneracy and the polarization $\alpha = [110]$, $\beta = [1\bar{1}0]$; unpolarized (unp).

Figure 1(a) shows a schematic of the calculated initial and final states of the X^{2-} transitions. On the left, we depict the dominant single-particle configurations, $h_0^1\, e_0^2\, e_1^1$ for the initial state and $e_0^1\, e_1^1$ for the final state. Many such states interact, producing the many particle energy ladder shown on the right. The initial many-body states are split by electron-hole exchange. The splitting between the uppermost initial states, E_b and E_c, is labeled Δ_1, and the splitting between the average of E_b and E_c and the doubly degenerate E_a is labeled Δ_0. The final many-body states are split by electron-electron exchange $2X_{ee}$ into a singlet state E_S and nearly degenerate triplet states E_T. For X^{2-}, the calculated Δ_1 and Δ_0 are comparable in magnitude (see Table I). For equal electron and hole orbitals, one would expect equal many-body spectra of X^{2-} and X^{2+}. This is not what the calculation reveals. Figure 1(b) shows the corresponding calculation for X^{2+}. The initial configuration, $h_0^2\, h_1^1\, e_0^1$, and the final configuration, $h_0^1\, h_1^1$, are analogous to those for X^{2-}. Despite this, the X^{2+} initial states are more similar to those of X^0 than X^{2-} as states E_b and E_c are only slightly split. Furthermore, the X^{2+} final states are not the same as those of X^{2-}: the degeneracy of the triplet is lifted, resulting in two singlets split by 2δ and a low energy doublet. The dramatic difference between X^{2-} and X^{2+} is highlighted (Table I) by the fact that the calculated $\Delta_1(X^{2-}) \simeq \Delta_0(X^{2-})$, yet $\Delta_1(X^{2+}) \ll \Delta_0(X^{2+})$.

Figure 1 allows an interpretation of the experimental results within the theoretical framework. All dots show the same fine-structure features. Figures 2(a) and 2(b) show measured X^{2-} PL spectra for two particular dots with close-to-average fine-structure splittings. For both InGaAs and InAs dots there are two groups of lines in the experiment, corresponding to transitions to the E_S and

TABLE I. Collection of experimental and theoretical values for Δ_0, Δ_1, given in μeV and X_{ee}, X_{hh}, δ in meV. The values in parentheses indicate calculations performed without the piezoelectricity. The experimental results are taken from two particular dots with close-to-average fine structure and exchange splittings.

	InGaAs		InAs	
	Experiment	Theory	Experiment	Theory
$\Delta_0(X^{2-})$	42	64 (65)	100	132 (155)
$\Delta_1(X^{2-})$	70	91 (96)	160	158 (210)
$\Delta_0(X^{2+})$	⋯	91 (95)	⋯	178 (180)
$\Delta_1(X^{2+})$	⋯	2 (7)	20	18 (17)
X_{ee}	2.25	3.66 (3.60)	5.08	5.31 (5.35)
X_{hh}	⋯	2.28 (2.00)	2.3	2.76 (2.91)
δ	⋯	1.28 (0.46)	1.34	1.00 (0.51)

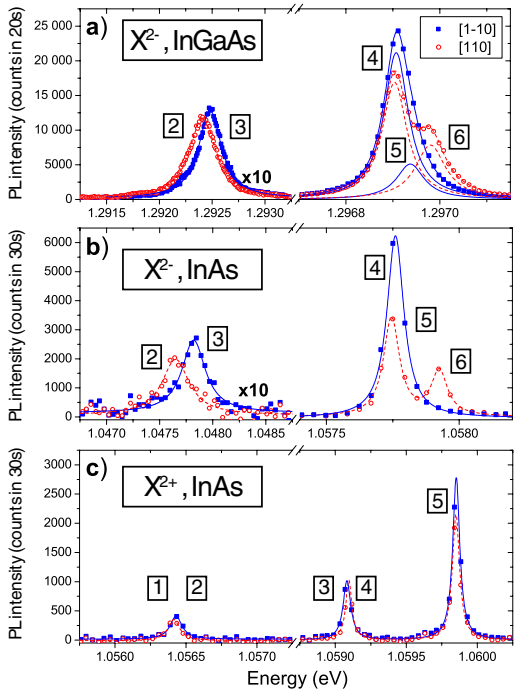

FIG. 2 (color online). Measured emission from doubly charged excitons at 4.2 K in two orthogonal linear polarizations. (a) X^{2-} for an InGaAs quantum dot; (b) X^{2-} for an InAs quantum dot; (c) X^{2+} for an InAs quantum dot. The transitions are labeled with the nomenclature of Fig. 1.

E_T final states. In the higher energy group, there are three PL lines, reflecting the presence of the three initial states. The uppermost PL line is [110] polarized and at lower energy there is a $[1\bar{1}0]$-polarized line. For each dot, these transitions are 100% polarized to within our experimental resolution of 5%, and the lowest energy line in the upper group is at most 20% polarized, lying almost at the same energy as the $[1\bar{1}0]$-polarized transition. We prove that these large fine-structure splittings arise in the initial and not in the final states by verifying the theoretical expectation that the E_T state is triply degenerate. We do this by observing weak recombination between the $h_0^1\, e_0^2\, e_1^1$ and e_0^2 (not $e_0^1\, e_1^1$) configurations where the final state has a closed S shell and is therefore a singlet. The PL however, Fig. 3, exhibits a large fine-structure splitting, with the same Δ_1 as for the open shell X^{2-} emissions in Fig. 2(a), proving that the triplet states are degenerate to within 10 μeV.

Several significant and surprising results emerge from the spectroscopy. First, Δ_1 for X^{2-} is considerably enhanced over that for the neutral exciton, X^0. This is the case for every dot we have looked at. For the InGaAs dots, the average (standard deviation) is $\Delta_1(X^0) = 26(12)$ μeV; $\Delta_1(X^{2-}) = 73(10)$. For the particular dots in Fig. 2, $\Delta_1(X^0)$ is experimentally 26($<$20) μeV, yet $\Delta_1(X^{2-})$ is 70(160) μeV for the InGaAs (InAs) quantum dot. Second, for X^{2-}, the usual relationship $\Delta_1 \ll \Delta_0$ is broken. In Fig. 2, we measure $\Delta_1/\Delta_0 = 1.6(1.7)$ for InAs (InGaAs) dots [17] leading to the unusual situation that states E_b and

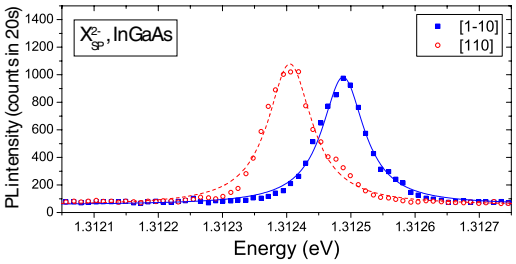

FIG. 3 (color online). Measured emission at 4.2 K in two orthogonal linear polarizations from the X^{2-} in a single InGaAs quantum dot at 4.2 K [different dot to Fig. 2(a)]. This particular X^{2-} emission is weak and strongly blueshifted relative to the main emission lines and arises from recombination of an S orbital hole and a P orbital electron.

E_a are almost degenerate. Again, this is the case for all the dots we have measured.

In the lower energy group of X^{2-} PL lines, there is always another polarized doublet; example data in Figs. 2(a) and 2(b) [18]. These lines arise from the transition from E_b and E_c to E_S and are split by $\Delta_1(X^{2-})$. However, the polarizations of the lower group are now reversed, with the $[1\bar{1}0]$- and *not* the [110]-polarized line at higher energy, as also observed for the transition to the closed shell in Fig. 3. This represents our third important experimental result.

We turn now to the X^{2+} PL which we have measured for the first time on an InAs dot; example data in Fig. 2(c). There is an unpolarized line with two fine-structure split doublets, each composed of two fully polarized lines, lying at lower energy. This is radically different to the X^{2-} PL, our fourth significant result. We point out several remarkable features of the X^{2+} spectrum. The most obvious is that the unpolarized emission line lies *above* the polarized emission lines. This is opposite to X^{2-} and also opposite to X^0, where the so-called dark states (unpolarized in the limit of zero magnetic field [1]) lie beneath the so-called bright states (linearly polarized emission). Second, the X^{2+} spectral features are located in an energy band of just 3.5 meV compared to 10.1 meV for X^{2-}. This is a surprise as hole-hole Coulomb energies are larger than electron-electron Coulomb energies. Finally, the doublets are separated by just $\Delta_1(X^{2+}) = 20$ μeV, which is small and only marginally enhanced over $\Delta_1(X^0)$ ($<$20 μeV), in complete contrast to $\Delta_1(X^{2-})$.

The theory (Fig. 4 and Table I) agrees very well with the experimental results. We present experimental results for the two particular dots in Fig. 2 but we stress that dot-to-dot fluctuations for the InGaAs dots in the 1.29–1.31 eV bandwidth are small, ± 10 μeV in the fine-structure splittings and ± 0.5 meV in the exchange energies. We have fewer data points for the InAs dots: two measured in complete detail gave fine-structure (exchange) splittings agreeing to within 10 μeV (0.5 meV); 10 dots measured without a full polarization analysis showed no hint of a splitting in the X^0 PL, implying that $\Delta_1(X^0) < 100$ μeV. Notably, the four

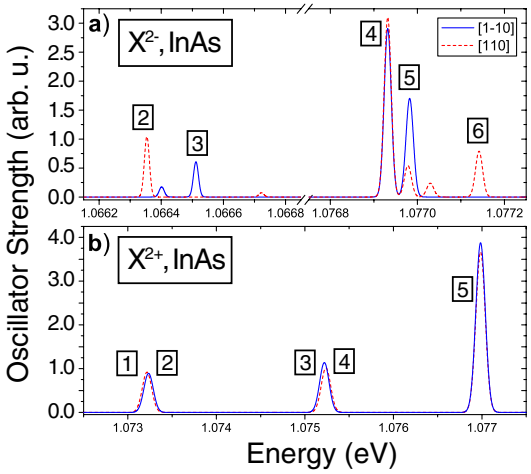

FIG. 4 (color online). Calculated emission spectra for (a) X^{2-} and (b) X^{2+} for an InAs dot. The emission lines have been broadened by 100 μeV for comparison with the experimental data of Fig. 2. The initial states are occupied according to Maxwell-Boltzmann statistics at 5 K. The weak lines at 1.06 640, 1.06 672, and 1.07 702 eV arise from occupation of an excited initial state configuration.

significant experimental results are paralleled by our theory. First, $\Delta_1(X^{2-})$ (91 μeV for the InGaAs dot and 158 μeV for the InAs dot) is significantly larger than $\Delta_1(X^0)$ (typically 10–50 μeV [3]). Second, $\Delta_1(X^{2-})$ is not significantly smaller than $\Delta_0(X^{2-})$ (as is typical for X^0) but similar (158 vs 132 μeV in InAs). We find that the near equivalence of $\Delta_0(X^{2-})$ and $\Delta_1(X^{2-})$ is a general feature in our calculations over a range of InGaAs and InAs dots. Third, the model also reproduces the polarizations of the X^{2-} PL: the calculated transitions are highly polarized but with reversed polarizations to E_S relative to E_T. Fourthly, the calculated X^{2+} spectrum also reproduces the most surprising experimental result, an unpolarized line at high energy with two lower-lying polarized doublets. The quantitative agreement between the energies defined and calculated theoretically and measured experimentally is very good with agreement to about $\sim$30% (Table I). For the InAs dots, inclusion of the piezoelectricity improves somewhat the agreement with experiment, particularly for $\Delta_1(X^{2-})$ and δ for X^{2+}. Further theoretical investigations would benefit from a full morphological characterization of the InAs dots.

Our theory, unlike the effective Hamiltonian approach, allows us to offer, in addition to the full calculation, some simple explanations. For X^{2-}, the fine structure mainly originates from the spin interaction between a hole in an S orbital and an electron in a P orbital (the two additional electrons form a closed shell in the S orbital). This interaction has a different symmetry than the one in the X^0 exciton where both carriers have an S-like envelope function character, resulting in a substantially different Δ_1. In the language of long- and short-range exchange, the large difference originates mainly from the long-range part of the exchange that can be seen as a dipole-dipole interaction, fundamentally different for an S-P exciton than for an S-S exciton. In the X^{2+} case, the initial state is similar to X^0 with a small value of Δ_1. This can be understood by the isotropic character of the envelope of the hole P orbital (Fig. 1 of Ref. [3]). X^{2+} is therefore closer to X^0, where both electron and hole envelopes are nearly isotropic, than to X^{2-} where the electron P wave function is highly anisotropic (Fig. 1 of Ref. [3]). The final state of the X^{2+} is drastically different to the final state of the X^{2-}. The two electrons in the X^{2-} final state follow the rules for spin-$\frac{1}{2}$ particles (triplet and singlet states) while the holes follow the addition of spin-$\frac{3}{2}$ particles. For dominantly heavy hole states, this leads to a twofold degenerate state with $J = 3$ and two singlets with $J = 0$ and $J = 2$.

To sum up, we have discovered new features in the fine structure of the doubly charged excitons, X^{2-} and X^{2+}, in both InAs and InGaAs quantum dots. For X^{2-}, the splitting between the linearly polarized doublet at high energy is close to the splitting between the polarized doublet and unpolarized line at lower energy ($\Delta_1 \sim \Delta_0$); very unusual behavior. For X^{2+}, the scaling reverts to type, $\Delta_1 \ll \Delta_0$, but the emission is radically reorganized due to a lifting of a degeneracy in the final state. There are two overriding points. First, we demonstrate a quantitative understanding of both energy splittings and selection rules of the X^{2-} and X^{2+} fine structure. Second, for our real, molecular-beam epitaxy-grown quantum dots, the lattice asymmetry and not the dot asymmetry makes the major contribution to the X^{2-} and X^{2+} fine structure.

We acknowledge financial support of this work from EPSRC (UK); DOE-SC-BES-DMS (under LAB-17), DAAD and SFB 631 (Germany), and SANDiE (EU).

[1] M. Bayer *et al.*, Phys. Rev. B **65**, 195315 (2002).
[2] A. Högele *et al.*, Phys. Rev. Lett. **93**, 217401 (2004).
[3] G. Bester *et al.*, Phys. Rev. B **67**, 161306 (2003).
[4] X. Li *et al.*, Science **301**, 809 (2003).
[5] C. Santori *et al.*, Phys. Rev. B **66**, 045308 (2002).
[6] R. M. Stevenson *et al.*, Nature (London) **439**, 179 (2006).
[7] N. Akopian *et al.*, Phys. Rev. Lett. **96**, 130501 (2006).
[8] R. Seguin *et al.*, Phys. Rev. Lett. **95**, 257402 (2005).
[9] E. A. Stinaff *et al.*, Science **311**, 636 (2006).
[10] B. Urbaszek *et al.*, Phys. Rev. Lett. **90**, 247403 (2003).
[11] K. Karrai *et al.*, Nature (London) **427**, 135 (2004).
[12] R. J. Young *et al.*, Phys. Rev. B **72**, 113305 (2005).
[13] R. J. Warburton *et al.*, Nature (London) **405**, 926 (2000).
[14] M. Ediger *et al.*, Appl. Phys. Lett. **86**, 211909 (2005).
[15] L.-W. Wang and A. Zunger, Phys. Rev. B **59**, 15 806 (1999).
[16] G. Bester *et al.*, Phys. Rev. Lett. **96**, 187602 (2006).
[17] $\Delta_1 \simeq 0.5\Delta_0$ has been reported for the charged biexciton $2X^{1-}$ in CdSe/ZnSe [I. A. Akimov *et al.*, Phys. Rev. B **71**, 075326 (2005)] but without a microscopic explanation.
[18] The increased linewidth of X^{2-} lines 2 and 3 is caused by fast relaxation of the $e_0^{\downarrow}\, e_1^{\downarrow}$ final state [13].